Quark distributions in nuclei

F. Catara[(1,2)] and M. Sambataro[(1)]
[(1)]*Istituto Nazionale di Fisica Nucleare, Sezione di Catania, Corso Italia 57, 95129 Catania, Italy*
[(2)]*Dipartimento di Fisica dell'Università, 95129 Catania, Italy*
(Received 11 December 1991)

By making use of a mapping procedure recently proposed, we construct the nucleon image of the one-body quark density operator in the framework of the nonrelativistic quark model of the nucleons. We evaluate the expectation value of this operator in the ground state of the doubly magic nuclei ^{4}He, ^{16}O, and ^{40}Ca described within the nuclear shell model. We analyze the role of quark exchanges between nucleons. We also investigate the effect on the quark density of short-range correlations in the nuclear wave functions as well as of variations in the nucleon size.

PACS number(s): 21.60.Cs, 21.90.+f

I. INTRODUCTION

A simple and yet effective way of describing baryons in terms of quarks is, at present, offered by the nonrelativistic quark model [1]. This model assumes that baryons are antisymmetrized clusters of three constituents quarks, each of them carrying color, spin, and isospin degrees of freedom. Quarks interact via a potential whose main terms are a confining and a hyperfine term. The former is responsible for the confinement of the quarks within the baryons, while the latter simulates the exchange of one gluon between quarks and is analogous to the electromagnetic potential describing the exchange of one photon in QED.

The nonrelativistic quark model has been taken as a starting point for a series of investigations searching for evidence of quark effects in nuclei. Examples of these investigations are those concerning the short-range part of the N-N interaction [2], the EMC effect [3,4], and the nuclear magnetic moments [5,6].

In spite of the simplicity of the model, the evaluation of quark observables even in very small nuclear systems, like $A=3$ systems, remains a quite difficult task due to the large number of particles involved. However, going to larger nuclear systems is important for a better understanding of the interplay between nucleonic and subnucleonic degrees of freedom.

Recently, we have pointed out a method to construct nucleon images of quark operators [7]. The method, which draws inspiration from similar techniques used in nuclear structure physics [8], is based on the concept of mapping and establishes a correspondence between spaces of three quark clusters and spaces of elementary nucleons. By *nucleon image* is meant an operator whose eigenspectrum in a space of A elementary nucleons is the same as that of the corresponding quark operator in a space of A clusters of quarks.

In order to be able to reproduce the very complicated quark-exchange dynamics, the nucleon image is expected to be much more complicated than the quark operator. Indeed, as we will see later, even when the latter is one body, its nucleon image can be A body if A is the number of nucleons of the system under study. One-,two-, . . . , A-body terms in the nucleon image take into account quark exchanges within one,two, . . . , A clusters, respectively.

Clearly, if one wished to use the full nucleon image, performing a calculation in the nucleon space would become as difficult as performing the equivalent calculation in the quark space. One would have only shifted from a quark picture of simple operators and complicated states to a nucleon picture of complicated operators and simple states. In both cases, calculations get difficult for $A>2$, so some approximations are required.

An interesting feature of our method is that it offers a natural way of selecting different levels of approximations in the operators, in correspondence to the different quark-exchange processes that one wishes to include in the calculations. Moreover, and more important, translating quark operators in the language of elementary nucleon operators allows one to evaluate quark observables directly in nuclear states constructed in the framework of conventional nuclear models.

In this paper, we will show an application of the mapping procedure starting from the one-body density quark operator. We will construct the one-body and two-body terms of its nucleon image. In terms of these, we will study the space distributions of quarks in doubly magic nuclei like ^{4}He, ^{16}O, and ^{40}Ca as they are predicted jointly by the shell model of the nucleus and the nonrelativistic quark model of the nucleon. The comparison between the calculations with the one-body and two-body nucleon terms will give us information on the role of quark exchanges in different nuclear systems. We will also examine the effects on the quark distributions of short-range correlations in the nuclear wave functions as well as of variations in the nucleon size.

The paper is organized as follows. In Sec. II we will review the main lines of the mapping procedure to construct nucleon images of quark operators. In Sec. III we will show an application of the procedure to the one-body quark density operator. In Sec. IV we will calculate quark distributions in nuclei and look into the effects of short-range correlations and nucleon size. Finally, in

Sec. V we will summarize the results and draw some conclusions.

II. THE PROCEDURE

The mapping procedure which will be used to construct the nucleon image of a quark operator is described in detail in Ref. [7]. Here, we will only discuss the main points.

We treat quarks by means of creation and annihilation operators $q_\eta^\dagger(\mathbf{r}), q_\eta(\mathbf{r})$, where $\eta \equiv \{c,s,t\}$ stands for the color c, the spin projection s, and the isospin projection t, respectively. They obey the usual fermion commutation relations

$$\{q_\eta(\mathbf{r}), q_{\eta'}^\dagger(\mathbf{r}')\} = \delta_{\eta\eta'}\delta(\mathbf{r}-\mathbf{r}') , \tag{1a}$$

$$\{q_\eta(\mathbf{r}), q_{\eta'}(\mathbf{r}')\} = \{q_\eta^\dagger(\mathbf{r}), q_{\eta'}^\dagger(\mathbf{r}')\} = 0 , \tag{1b}$$

where $\{A,B\} = AB + BA$.

Restricting ourselves to protons and neutrons, we only introduce up and down quarks, which are characterized by isospin $\frac{1}{2}$ and projections $t=\frac{1}{2}$ and $t=-\frac{1}{2}$, respectively. By means of these operators, we construct operators $N_{\sigma\tau}^\dagger(\mathbf{R})$ that create clusters of three quarks in a color singlet state with total spin $\frac{1}{2}$, isospin $\frac{1}{2}$, and projections σ and τ, respectively, and with center of mass in $\mathbf{R}$. It is

$$\begin{aligned} N_{\sigma\tau}^\dagger(\mathbf{R}) = \frac{1}{3!\sqrt{2}} \sum_{c_1c_2c_3} \epsilon_{c_1c_2c_3} \sum_{s_1s_2s_3} \sum_{S} (\tfrac{1}{2}s_1\tfrac{1}{2}s_2|Ss_1+s_2)(Ss_1+s_2\tfrac{1}{2}s_3|\tfrac{1}{2}\sigma) \\ \times \sum_{t_1t_2t_3} \sum_{T} (\tfrac{1}{2}t_1\tfrac{1}{2}t_2|Tt_1+t_2)(Tt_1+t_2\tfrac{1}{2}t_3|\tfrac{1}{2}\tau) \\ \times \int d\mathbf{r}_1 d\mathbf{r}_2 d\mathbf{r}_3 \delta(\mathbf{r}_1+\mathbf{r}_2+\mathbf{r}_3-3\mathbf{R}) \Omega(\mathbf{r}_1,\mathbf{r}_2,\mathbf{r}_3;\mathbf{R}) q_{\eta_1}^\dagger(\mathbf{r}_1) q_{\eta_2}^\dagger(\mathbf{r}_2) q_{\eta_3}^\dagger(\mathbf{r}_3) . \end{aligned} \tag{2}$$

Here, $\epsilon_{c_1c_2c_3}$ is the totally antisymmetric tensor of rank 3, and $\Omega(\mathbf{r}_1,\mathbf{r}_2,\mathbf{r}_3;\mathbf{R})$ describes the spatial distribution of the quarks in the cluster and is fully symmetric under permutations of $\mathbf{r}_1,\mathbf{r}_2,\mathbf{r}_3$.

We take $\Omega(\mathbf{r}_1,\mathbf{r}_2,\mathbf{r}_3;\mathbf{R})$ to be the product of three Gaussians in the coordinates of the quarks relative to the center of mass of the cluster

$$\Omega(\mathbf{r}_1,\mathbf{r}_2,\mathbf{r}_3;\mathbf{R}) = \frac{3^{9/4}\gamma^3}{\pi^{3/2}} \exp\{-\tfrac{1}{2}\gamma^2[(\mathbf{r}_1-\mathbf{R})^2+(\mathbf{r}_2-\mathbf{R})^2+(\mathbf{r}_3-\mathbf{R})^2]\} . \tag{3}$$

The normalization is chosen such that

$$\langle 0_q | N_{\sigma\tau}(\mathbf{R}) N_{\sigma'\tau'}^\dagger(\mathbf{R}') | 0_q \rangle = \delta_{\sigma\sigma'}\delta_{\tau\tau'}\delta(\mathbf{R}-\mathbf{R}') , \tag{4}$$

where $|0_q\rangle$ represents the vacuum of the quark space.

We notice that although they describe nucleons, the cluster operators (2) do not obey fermion commutation relations of the type (1) because of their composite nature.

We call N^A the space of nucleon clusters that is spanned by states of the form

$$N_{\sigma_1\tau_1}^\dagger(\mathbf{R}_1) N_{\sigma_2\tau_2}^\dagger(\mathbf{R}_2) \cdots N_{\sigma_A\tau_A}^\dagger(\mathbf{R}_A) |0_q\rangle , \tag{5}$$

Similarly, we introduce creation and annihilation operators $n_{\sigma\tau}^\dagger(\mathbf{R}), n_{\sigma\tau}(\mathbf{R})$ for elementary nucleons. They do obey commutation relations of the type (1). We call n^A the space spanned by the states

$$n_{\sigma_1\tau_1}^\dagger(\mathbf{R}_1) n_{\sigma_2\tau_2}^\dagger(\mathbf{R}_2) \cdots n_{\sigma_A\tau_A}^\dagger(\mathbf{R}_A) |0_n\rangle , \tag{6}$$

where $|0_n\rangle$ is the vacuum of the nucleon space. States (6) are formally obtained from states (5) by replacing cluster creation operators $N_{\sigma\tau}^\dagger(\mathbf{R})$ with nucleon creation operators $n_{\sigma\tau}^\dagger(\mathbf{R})$ and the quark vacuum with the nucleon vacuum. This correspondence is such that the orthogonality relations between corresponding states are not preserved.

The procedure for constructing a nucleon image of a quark operator $\hat{W}_q$ has two main steps. In the first, one defines a new quark operator $\hat{W}_q^{(A)}$ exactly equivalent to $\hat{W}_q$ within a given quark space $N^{(A)}$ and such that it does not lead out of this space. In the second step, one constructs a nucleon operator $\hat{\hat{W}}_n^{(A)}$ whose action on a state of $n^{(A)}$ is formally identical to that of the operator $\hat{W}_q^{(A)}$ on the corresponding state of $N^{(A)}$. This guarantees that if $|\Psi_q\rangle$ is an eigenstate of $\hat{W}_q^{(A)}$ in $N^{(A)}$ with a given eigenvalue, the corresponding state $|\Psi_n\rangle$ in $n^{(A)}$ is also an eigenstate of $\hat{\hat{W}}_n^{(A)}$ with the same eigenvalue.

As a consequence of the nonunitarity of the correspondence between states (5) and (6), the nucleon operator so constructed is, in general, non-Hermitian. However, it was shown in Ref. [7] that, by means of an appropriate transformation, this undesired feature can be removed.

As a general result, the nucleon operator which is constructed is a sum of one-,two-, . . . , A-body terms if A is the number of clusters in the system under study, i.e.,

$$\hat{\hat{W}}_n^{(A)} = \hat{W}_n^{(1)} + \hat{W}_n^{(2)} + \cdots + \hat{W}_n^{(A)} . \tag{7}$$

Such a complicated structure is determined by the need for simulating in a space of A elementary nucleons the complicated quark-exchange dynamics within the A clusters. Each of the A terms contributing to the formation of the nucleon image is linked to a different physical process, the one-body term reflecting only the quark dynamics within one cluster, the two-body term the quark exchanges between two clusters, etc.

Of course, evaluating the exact nucleon image when A

is large becomes quite difficult, and therefore some approximations are required. By limiting ourselves to processes which involve at most exchanges of quarks between two nucleons, only the one-body and two-body terms of (7) are needed. These operators are characterized by the following matrix elements in the n^1 and n^2 spaces [7]:

$$\langle 0_n | n_{\sigma'\tau'}(\mathbf{R}')\hat{W}_n^{(1)} n^\dagger_{\sigma\tau}(\mathbf{R})|0_n\rangle = \langle 0_q | N_{\sigma'\tau'}(\mathbf{R}')\hat{\mathrm{W}}_{\mathrm{q}} \mathrm{N}^\dagger_{\sigma\tau}(\mathbf{R})|0_{\mathrm{q}}\rangle \tag{8}$$

and

$$\langle 1,2|\hat{W}_n^{(2)}|1',2'\rangle_n = \int_{1^*,2^*,\bar{1},\bar{2}} \langle 1,2|1^*,2^*\rangle_q^{-1/2} \langle 1^*,2^*|\hat{W}_q|\bar{1},\bar{2}\rangle_q \langle \bar{1},\bar{2}|1',2'\rangle_q^{-1/2} - \langle 1,2|\hat{W}_n^{(1)}|1',2'\rangle_n \ , \tag{9}$$

where $i \equiv \{\mathbf{R}_i, \sigma_i, \tau_i\}$,

$$N^\dagger_{\sigma_1\tau_1}(\mathbf{R}_1)\mathrm{N}^\dagger_{\sigma_2\tau_2}(\mathbf{R}_2)|0_{\mathrm{q}}\rangle \equiv |1,2\rangle_{\mathrm{q}} \ , \tag{10}$$

$$n^\dagger_{\sigma_1\tau_1}(\mathbf{R}_1)\mathrm{n}^\dagger_{\sigma_2\tau_2}(\mathbf{R}_2)|0_{\mathrm{n}}\rangle \equiv |1,2\rangle_{\mathrm{n}} \ , \tag{11}$$

and where the symbol $\int_{i,\ldots}$ means integration (summation) over continuous (discrete) variables $i,\ldots$.

In the following we will show practical realizations of these nucleon operators.

III. THE NUCLEON IMAGE OF THE ONE-BODY QUARK DENSITY OPERATOR

The starting point for the application of the mapping procedure discussed in the previous section will be the one-body quark density operator

$$\hat{\rho}_q(\mathbf{r}) = \sum_\eta q^\dagger_\eta(\mathbf{r}) q_\eta(\mathbf{r}) \ . \tag{12}$$

According to Eq. (8), the one-body nucleon image is

$$\hat{\rho}_n^{(1)}(\mathbf{r}) = \sum_{\sigma\tau\sigma'\tau'} \int d\mathbf{R}\, d\mathbf{R}' \langle 0_q | N_{\sigma\tau}(\mathbf{R})\hat{\rho}_q(\mathbf{r}) N^\dagger_{\sigma'\tau'}(\mathbf{R}')|0_q\rangle \times n^\dagger_{\sigma\tau}(\mathbf{R}) n_{\sigma'\tau'}(\mathbf{R}') \ , \tag{13}$$

and since

$$\langle 0_q | N_{\sigma\tau}(\mathbf{R})\hat{\rho}_q(\mathbf{r}) N^\dagger_{\sigma'\tau'}(\mathbf{R}')|0_q\rangle = \delta_{\sigma,\sigma'}\delta_{\tau,\tau'}\delta(\mathbf{R}-\mathbf{R}') \frac{\gamma^3 3^{5/2}}{2^{3/2}\pi^{3/2}} e^{-(3/2)\gamma^2(\mathbf{R}-\mathbf{r})^2} \ , \tag{14}$$

it is also

$$\hat{\rho}_n^{(1)}(\mathbf{r}) = \sum_{\sigma\tau} \int d\mathbf{R} \frac{\gamma^3 3^{5/2}}{2^{3/2}\pi^{3/2}} e^{-(3/2)\gamma^2(\mathbf{R}-\mathbf{r})^2} n^\dagger_{\sigma\tau}(\mathbf{R}) n_{\sigma\tau}(\mathbf{R}) \ . \tag{15}$$

Equation (14) gives the quark distribution in a free nucleon.

We notice that in the limit $\gamma \to \infty$, corresponding to pointlike clusters,

$$\hat{\rho}_n^{(1)}(\mathbf{r}) \to 3 \sum_{\sigma\tau} n^\dagger_{\sigma\tau}(\mathbf{r}) n_{\sigma\tau}(\mathbf{r}) \ , \tag{16}$$

which is three times the usual one-body nucleon density operator. For any finite value of γ, the quark distribution calculated with the operator (15) is given by the nucleon distribution folded with the quark distribution in a free nucleon.

The operator (15) does not take into account any quark-exchange process between nucleons. The simplest of these processes, the exchange of quarks between two nucleons, can be described in terms of the two-body term

$$\hat{\rho}_n^{(2)}(\mathbf{r}) = \tfrac{1}{4} \int_{1,2,1',2'} \langle 1,2|\hat{\rho}_n^{(2)}(\mathbf{r})|1',2'\rangle_n n_1^\dagger n_2^\dagger n_{2'} n_{1'} \ . \tag{17}$$

The calculation of the two-body matrix elements appearing in this operator, using Eq. (9), is rather involved. We illustrate in the following how it has been carried out.

It is useful to introduce a more compact notation, similar to that of Ref. [4], and rewrite the cluster creation operator as

$$N^\dagger_{\sigma_i\tau_i}(\mathbf{R}_i) \equiv N_i^\dagger \equiv C^i_{\mu_1\mu_2\mu_3} q^{(r)\dagger}_{\mu_1} q^{(g)\dagger}_{\mu_2} q^{(b)\dagger}_{\mu_3} \ , \tag{18}$$

where $\mu \equiv \{s,t,\mathbf{r}\}$ and r,g,b stand for the colors red, green, and blue of the quarks;

$$C^i_{\mu_1\mu_2\mu_3} = \frac{1}{\sqrt{18}} D(s_1t_1,s_2t_2,s_3t_3;\sigma_i\tau_i)\delta(\mathbf{r}_1+\mathbf{r}_2+\mathbf{r}_3-3\mathbf{R}_i)\Omega(\mathbf{r}_1,\mathbf{r}_2,\mathbf{r}_3;\mathbf{R}_i) \ , \tag{19}$$

with

$$D(s_1t_1,s_2t_2,s_3t_3;\sigma\tau) = \tfrac{1}{2}\left[\sum_S (\tfrac{1}{2}s_1\tfrac{1}{2}s_2|Ss_1+s_2)(Ss_1+s_2\tfrac{1}{2}s_3|\tfrac{1}{2}\sigma) \times \sum_T (\tfrac{1}{2}t_1\tfrac{1}{2}t_2|Tt_1+t_2)(Tt_1+t_2\tfrac{1}{2}t_3|\tfrac{1}{2}\tau) + \mathrm{perm}(1,2,3) \right] \ , \tag{20}$$

and it is understood that repeated indices imply summations (integrations) over discrete (continuous) variables. However, when writing the one-body quark density operator (12) in the new notation, i.e.,

$$\hat{\rho}_q(\mathbf{r})=q_\mu^{(r)\dagger}q_\mu^{(r)}+q_\mu^{(g)\dagger}q_\mu^{(g)}+q_\mu^{(b)\dagger}q_\mu^{(b)} , \tag{21}$$

the coordinate $\mathbf{r}$ of the quark does not have to be integrated.

By limiting ourselves to one of the three terms of (21), for instance the red one, we have

$$\langle 0_q|N_2N_1q_\mu^{(r)\dagger}q_\mu^{(r)}N_{1'}^\dagger N_{2'}^\dagger|0_q\rangle=\langle 0_q|N_2\{N_1,q_\mu^{(r)\dagger}\}\{q_\mu^{(r)},N_{1'}^\dagger\}N_{2'}^\dagger|0_q\rangle-(1'\leftrightarrow 2')-(1\leftrightarrow 2)+(1'\leftrightarrow 2',1\leftrightarrow 2) . \tag{22}$$

Moreover,

$$\langle 0_1|N_2\{N_1,q_\mu^{(r)\dagger}\}\{q_\mu^{(r)},N_{1'}^\dagger\}N_{2'}^\dagger|0_q\rangle=C^1_{\mu\nu_2\nu_3}C^2_{\epsilon_1\epsilon_2\epsilon_3}(C^{1'}_{\mu\nu_2\nu_3}C^{2'}_{\epsilon_1\epsilon_2\epsilon_3}-C^{1'}_{\mu\nu_2\epsilon_3}C^{2'}_{\epsilon_1\epsilon_2\nu_3}-C^{1'}_{\mu\epsilon_2\nu_3}C^{2'}_{\epsilon_1\nu_2\epsilon_3}+C^{1'}_{\mu\epsilon_2\epsilon_3}C^{2'}_{\epsilon_1\nu_2\nu_3}) . \tag{23}$$

This formula is well illustrated in terms of the diagrams of Fig. 1 which are self-explaining. The evaluation of the single diagrams gives the results which are listed below.

Diagram (1a):

$$C^1_{\mu\nu_2\nu_3}C^2_{\epsilon_1\epsilon_2\epsilon_3}C^{1'}_{\mu\nu_2\nu_3}C^{2'}_{\epsilon_1\epsilon_2\epsilon_3}=\delta_{1,1'}\delta_{2,2'}\left[\frac{\gamma^2 3}{2\pi}\right]^{3/2}e^{-(3/2)\gamma^2(\mathbf{R}-\mathbf{r})^2} . \tag{24}$$

Diagrams (1b)+(1c):

$$\begin{aligned}C^1_{\mu\nu_2\nu_3}&C^2_{\epsilon_1\epsilon_2\epsilon_3}(C^{1'}_{\mu\nu_2\epsilon_3}C^{2'}_{\epsilon_1\epsilon_2\nu_3}+C^{1'}_{\mu\epsilon_2\nu_3}C^{2'}_{\epsilon_1\nu_2\epsilon_3})\\ &=\frac{1}{18^2}D(st,s_{\nu_2}t_{\nu_2},s_{\nu_3}t_{\nu_3};\sigma_1,\tau_1)D(s_{\epsilon_1}t_{\epsilon_1},s_{\epsilon_2}t_{\epsilon_2},s_{\epsilon_3}t_{\epsilon_3};\sigma_2,\tau_2)\\ &\quad\times[D(st,s_{\nu_2}t_{\nu_2},s_{\epsilon_3}t_{\epsilon_3};\sigma_{1'},\tau_{1'})D(s_{\epsilon_1}t_{\epsilon_1},s_{\epsilon_2}t_{\epsilon_2},s_{\nu_3}t_{\nu_3};\sigma_{2'},\tau_{2'})+D(st,s_{\epsilon_2}t_{\epsilon_2},s_{\nu_3}t_{\nu_3};\sigma_{1'},\tau_{1'})D(s_{\epsilon_1}t_{\epsilon_1},s_{\nu_2}t_{\nu_2},s_{\epsilon_3}t_{\epsilon_3};\sigma_{2'},\tau_{2'})]\\ &\quad\times\frac{3^6\gamma^6}{7^{3/2}\pi^3}e^{-(3/4)\gamma^2(\mathbf{R}-\mathbf{R}')^2}e^{-(3/16)\gamma^2(\mathbf{R}+\mathbf{R}')^2}e^{-(12/7)\gamma^2[(3/8)(\mathbf{R}+\mathbf{R}')-\mathcal{R}+\mathbf{r}]^2}\delta(\mathcal{R}-\mathcal{R}') .\end{aligned} \tag{25}$$

Diagram (1d):

$$\begin{aligned}C^1_{\mu\nu_2\nu_3}C^2_{\epsilon_1\epsilon_2\epsilon_3}C^{1'}_{\mu\epsilon_2\epsilon_3}C^{2'}_{\epsilon_1\nu_2\nu_3}&=\frac{1}{18^2}D(st,s_{\nu_2}t_{\nu_2},s_{\nu_3}t_{\nu_3};\sigma_1,\tau_1)D(s_{\epsilon_1}t_{\epsilon_1},s_{\epsilon_2}t_{\epsilon_2},s_{\epsilon_3}t_{\epsilon_3};\sigma_2,\tau_2)\\ &\quad\times D(st,s_{\epsilon_2}t_{\epsilon_2},s_{\epsilon_3}t_{\epsilon_3};\sigma_{1'},\tau_{1'})D(s_{\epsilon_1}t_{\epsilon_1},s_{\nu_2}t_{\nu_2},s_{\nu_3}t_{\nu_3};\sigma_{2'},\tau_{2'})\\ &\quad\times\frac{3^6\gamma^6}{2^3\pi^3}e^{-(3/4)\gamma^2(\mathbf{R}+\mathbf{R}')^2}e^{-(3/16)\gamma^2(\mathbf{R}-\mathbf{R}')^2}e^{-3\gamma^2[(3/4)(\mathbf{R}+\mathbf{R}')+\mathcal{R}-\mathbf{r}]^2}\delta(\mathcal{R}-\mathcal{R}') .\end{aligned} \tag{26}$$

In the previous formulas, $\mathbf{R}=\mathbf{R}_1-\mathbf{R}_2,\mathbf{R}'=\mathbf{R}_{1'}-\mathbf{R}_{2'},\mathcal{R}=\mathbf{R}_1+\mathbf{R}_2$, and $\mathcal{R}'=\mathbf{R}_{1'}+\mathbf{R}_{2'}$.

Concerning the two-cluster overlaps, we simply notice that

$$\langle 0_q|N_2N_1N_{1'}^\dagger N_{2'}^\dagger|0_q\rangle=\tfrac{1}{6}\int d\mathbf{r}\langle 0_q|N_2N_1\hat{\rho}_q(\mathbf{r})N_{1'}^\dagger N_{2'}^\dagger|0_q\rangle . \tag{27}$$

By including only processes where quarks are exchanged at most between two nucleons simultaneously, the nucleon image of the one-body quark density operator is therefore the one-body plus two-body operator

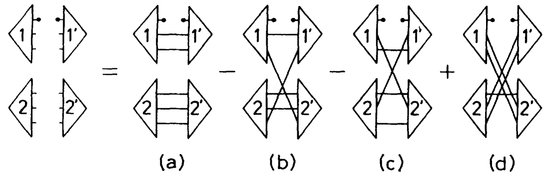

FIG. 1. Diagrams illustrating Eq. (23).

$$\hat{\rho}_n(\mathbf{r})=\hat{\rho}_n^{(1)}(\mathbf{r})+\hat{\rho}_n^{(2)}(\mathbf{r}) . \tag{28}$$

IV. QUARK DISTRIBUTIONS IN ^{4}He, ^{16}O, and ^{40}Ca

We have evaluated the expectation values of the operators (15) and (17) in the ground state of three doubly magic nuclei: ^{4}He, ^{16}O, and ^{40}Ca. This ground state has been described first within a pure nuclear shell model with harmonic-oscillator wave functions. Results are illustrated in Figs. 2–4, where the solid line refers to the operator (28), while the dashed line refers only to the one-body term (15). In these calculations, the harmonic-oscillator parameter γ of the quark wave function (3) has been taken equal to 1.25 fm^{-1}, corresponding to a nucleon r.m.s.r. (root mean square radius) of 0.8 fm. The equivalent harmonic-oscillator parameter for the nuclear wave functions has been chosen as 0.77 fm^{-1} for ^{4}He, 0.63 fm^{-1} for ^{16}O, and 0.50 fm^{-1} for ^{40}Ca. This choice guarantees the correct r.m.s.r. of these nuclei.

Figures 2–4 clearly show the non-negligible effect of quark-exchange processes in determining the quark distributions. This effect gets larger for the heavier nuclei

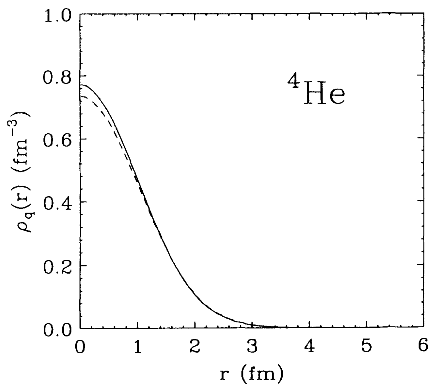

FIG. 2. Quark distribution in ^{4}He as predicted by the nonrelativistic quark model in conjunction with a pure nuclear shell model with harmonic-oscillator wave functions. The solid line is the expectation value of the operator (28) in the nuclear ground state. The dashed line shows the contribution of the one-body part (15) only. The normalization is chosen such that $\int r^2 dr\, \rho_1(r) = 1$.

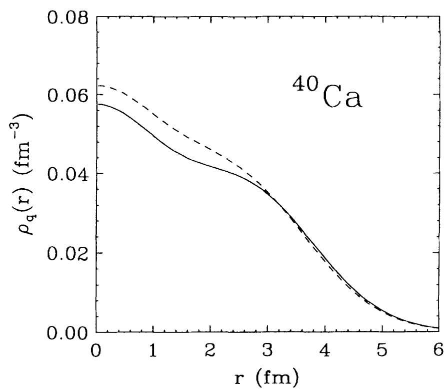

FIG. 4. The same as Fig. 2 but for ^{40}Ca.

and increases for decreasing values r of the distance from the origin of the system.

The calculations shown so far describe nuclei as systems of independent particles. However, quark exchange being intrinsically a short-range process, one can expect that hard-core correlations between interacting nucleons can significantly alter the results. We have investigated to what degree this happens by introducing a correlation function of the type

$$f(\mathbf{R}_1,\mathbf{R}_2) = 1 - e^{-a|\mathbf{R}_1-\mathbf{R}_2|^2} \tag{29}$$

and replacing states (10) with states

$$f(\mathbf{R}_1,\mathbf{R}_2) N^{\dagger}_{\sigma_1\tau_1}(\mathbf{R}_1) N^{\dagger}_{\sigma_2\tau_2}(\mathbf{R}_2)|0_q\rangle \ . \tag{30}$$

Obviously, the results concerning the one-body nucleon operator are not affected by these changes. With reference to the two-body term, one observes the modifications that are quantified in Figs. 5 and 6 for ^{4}He and ^{16}O, respectively. Here, the solid line refers to the quark distributions calculated without hard-core correlations, while the long-dashed and short-dashed lines are the results obtained by using two-cluster states with $a=4$ and $a=2$, respectively.

The short-range repulsion is found to cause a decrease of the quark density at small r and a consequent increase at large r. This effect is the more evident for smaller values of the parameter a of the correlation function (29), i.e., the more intense the short-range repulsion is. Even for a rather intense repulsion, however, the effect is not sufficient to alter drastically the quark distribution.

As a final point, we have calculated the variations of the quark density caused by changes in nucleon size. In Fig. 7 one sees the expectation values of the operators (15) (positive sector) and (17) (negative sector) for $\gamma=1.11$ fm^{-1} (long-dashed line), $\gamma=1.25$ fm^{-1} (solid line), and $\gamma=1.43$ fm^{-1} (short-dashed line) in the case of ^{16}O. These cases correspond to nucleon r.m.s.r. of 0.9, 0.8, and 0.7 fm, respectively. For increasing nucleon radii (and constant nuclear radius) one observes a growing of the exchange effects at small values of r, while the expectation of the one-body term stays rather constant. Thus, the global effect is a reduction of quark density similar to that observed in the introduction of the correlation factor (29) simulating a short-range repulsion (Fig. 6). In this case, however, the effect is only due to the antisymmetrization of the nuclear wave functions with respect to quarks.

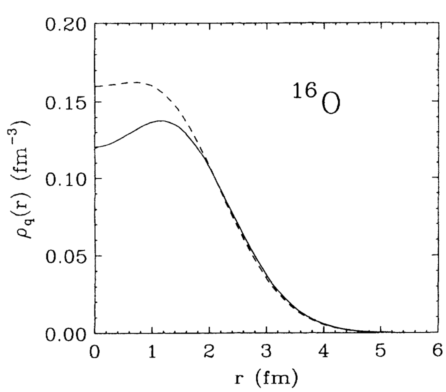

FIG. 3. The same as Fig. 2 but for ^{16}O.

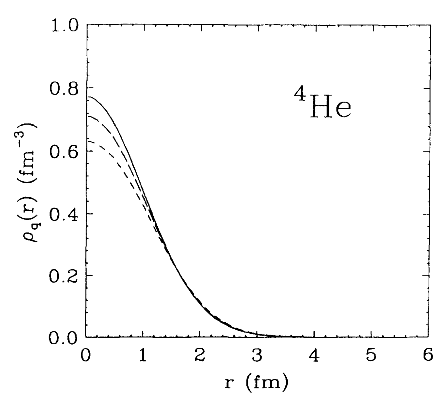

FIG. 5. Effects of short-range nuclear correlations on the quark distribution of ^{4}He. Solid line: no correlations. Long-dashed line: $a=4$ fm^{-1} in the function (29). Short-dashed line: $a=2$ fm^{-2} in (29). The normalization is chosen such that $\int r^2 dr\, \rho_q(r) = 1$.

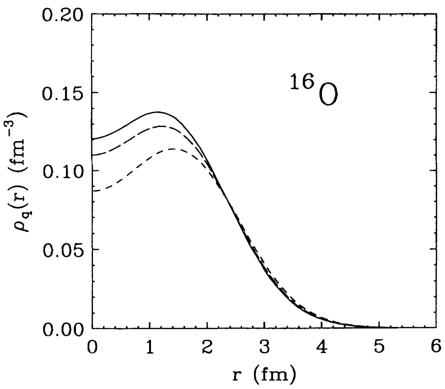

FIG. 6. The same as in Fig. 5 but for ^{16}O.

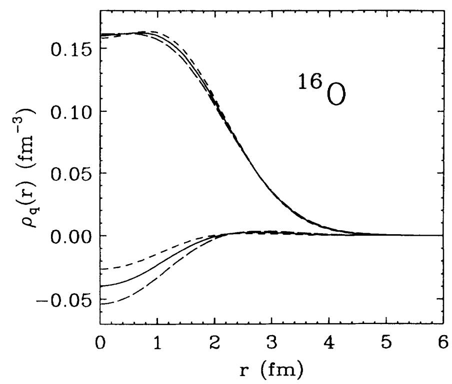

FIG. 7. Expectation values of the one-body term (15) (positive sector) and of the two-body term (17) (negative sector) in the ground state of ^{16}O. Solid line: $\gamma=1.25$ fm^{-1} ($\langle r^2\rangle^{1/2}=0.8$ fm). Long-dashed line: $\gamma=1.11$ fm^{-1} ($\langle r^2\rangle^{1/2}=0.9$ fm). Short-dashed line: $\gamma=1.43$ fm^{-1} ($\langle r^2\rangle^{1/2}=0.7$ fm).

V. SUMMARY AND CONCLUSIONS

In this paper we have discussed a method for constructions nucleon images of quark operators. As an application, we have studied the one-body quark density operator. We have derived the one-body and two-body terms of its nucleon image and we have calculated the space distributions of quarks in ^4He, ^{16}O, and ^{40}Ca as predicted jointly by the shell model of the nucleus and the quark-cluster model of the nucleon. The quark distribution that one calculates corresponding to the one-body term turns out to be equal to the distribution of elementary nucleons predicted by the nuclear shell model folded with the distribution of quarks inside a free nucleon. The contribution of the two-body term takes into account exchanges of quarks between two different nucleons.

We have performed two series of calculations, the first assuming an independent particle approach, and the second introducing short-range correlations between nucleons. We have found that quark exchange produces sizable effects on the quark distributions, larger for the heavier elements and increasing for decreasing values of the distance r from the origin of the reference system. We have also seen that short-range correlations can appreciably modify the quark distributions in the sense of shifting them towards large values of r, without, however, causing drastic alterations. Finally, we have analyzed the variations of the quark distributions caused by changes in the nucleon size and found that an increase in this size gives rise to effects similar to those produced by the short-range correlations.

Previous investigations of spatial distributions of quarks in nuclei within the nonrelativistic quark-cluster model have been performed by Hoodbhoy [9], but only for $A=3$ systems. It is interesting to observe that his result for ^3He is quite similar to that shown in Fig. 2 for ^4He. In his analysis, as in ours, processes involving the simultaneous exchange of quarks between three nucleons have been neglected.

To our knowledge, one can find in the literature only one other calculation of quark observables in nuclear systems of comparable "size" to those studied in this paper. This is contained in the recent work of Yamauchi, Buchmann, Faessler, and Arima [6] on quark-exchange currents in nuclei. Their inspiring philosophy has been the same as ours [7], namely, that of constructing an effective nucleon operator starting from a quark operator, and their procedure has been based on the resonating group method.

So far, we have looked into space distributions of quarks in nuclei. With only a few changes in the formalism we are in a position to examine also quark momentum distributions. The importance of quark exchanges in modifying these distributions and the consequences that these can have on the nucleon structure function have already been pointed out in connection with the EMC effect [3,4]. However, these calculations have concerned either very small systems, namely, $A=3$ systems [3], or nuclear matter [4]. Our formalism allows the extension of this analysis to more interesting intermediate situations. We expect that the non-negligible role of quark exchanges found in the coordinate representation will be confirmed in the momentum representation, and we therefore hope that these calculations can provide a significant contribution to the understanding of this interesting nuclear phenomenon.

[1] N. Isgur and G. Karl, Phys. Rev. D **18**, 4187 (1978); **19**, 2653 (1979); **20**, 1191 (1979); **21**, 3175 (1980); M. Oka and K. Yazaki, Phys. Lett. **90B**, 41 (1980); Nucl. Phys. **A402**, 477 (1983); in *Quarks and Nuclei,* International Review of Nuclear Physics Series, Vol. 1, edited by W. Weise (World Scientific, Singapore, 1984), p. 489; A. Faessler, F. Fernandez, G. Lübeck, and K. Shimizu, Nucl. Phys. **A402**, 555 (1983); H. J. Lipkin, *ibid.* **A446**, 409c (1985); B. Silvestre-Brac and C. Cignoux, Phys. Rev. D **32**, 743 (1985); Y. Yamauchi, R. Yamamoto, and M. Wakamatsu, Nucl. Phys. **A443**, 628 (1985).

[2] For reviews, see F. Myrher and J. Wroldsen, Rev. Mod. Phys. **60**, 629 (1988); K. Shimizu, Rep. Prog. Phys. **52**, 1 (1989).

[3] P. Hoodbhoy and R. L. Jaffe, Phys. Rev. D **35**, 113 (1987).
[4] Arifuzzaman, S. H. Hasan, and P. Hoodbhoy, Phys. Rev. C **38**, 498 (1988).
[5] M. Katô, W. Bentz, K. Shimizu, and A. Arima, Phys. Rev. C **42**, 2672 (1990).
[6] Y. Yamauchi, A. Buchmann, A. Faessler, and A. Arima, Nucl. Phys. **A526**, 495 (1991).
[7] F. Catara and M. Sambataro, Nucl. Phys. **A535**, 605 (1991); in *Perspectives on Theoretical Nuclear Physics, Proceedings of the Meeting on Perspectives on Theoretical Nuclear Physics,* Cortona, Italy, 1989, edited by L. Bracci *et al.* (ETS Editrice, Pisa, 1990), p. 233; in *Understanding the Variety of Nuclear Excitations, Proceedings of the 3rd International Spring Seminar on Nuclear Physics,* Ischia, Italy, 1990, edited by A. Covello (World Scientific, Singapore, 1991), p. 99.
[8] M. Sambataro, Phys. Rev. Lett. **57**, 1503 (1986); Phys. Rev. C **35**, 1530 (1987); **37**, 2186 (1988); **37**, 2199 (1988).
[9] P. Hoodbhoy, Nucl. Phys. **A465**, 637 (1987).